Journal of Magnetism and Magnetic Materials 321 (2009) 3335–3341

Contents lists available at ScienceDirect

Journal of Magnetism and Magnetic Materials

journal homepage: www.elsevier.com/locate/jmmm

Ferromagnetism of epitaxially grown $CaRu_{1-x}M_xO_3$ (M = Ti, Mn) films

S. Taniguchi [a], M. Ogawara [a], N. Fukuoka [a], S. Mizusaki [a], Y. Nagata [a,*], Y. Noro [b], H. Samata [c]

[a] College of Science and Engineering, Aoyama Gakuin University, Fuchinobe, Sagamihara, Kanagawa 229-8558, Japan
[b] Kawazoe Frontier Technologies, Co. Ltd., Sakae, Yokohama, Kanagawa 931-113, Japan
[c] Graduate School of Maritime Science, Kobe University, Fukaeminami, Higashinada, Kobe, Hyogo 658-0022, Japan

ARTICLE INFO

Article history:
Received 30 March 2009
Received in revised form
29 May 2009
Available online 18 June 2009

PACS:
68.55.−a
75.70.−I
75.50.Dd
75.70.Ak
75.70.Cn

Keywords:
Epitaxial film
Spin coating
Ruthenium oxides
Magnetism
Conductivity

ABSTRACT

Epitaxial thin films of $CaRu_{1-x}M_xO_3$ (M = Ti, Mn) were fabricated on a (0 0 1)-$SrTiO_3$ substrate by spin-coat method using organometallic solutions (metal alkoxides). Results of X-ray diffraction and transmission electron microscopy indicate that the epitaxial films were grown pseudomorphically so as to align the [0 0 l] axis of the $CaRu_{1-x}M_xO_3$ films perpendicular to the (0 0 1) plane of the $SrTiO_3$ substrate. Ferromagnetism and metal–insulator transition are induced by the substitution of transition metal ions. The occurrence of ferromagnetism was explained qualitatively assuming a $TiRu_6$ cluster model for $CaRu_{1-x}Ti_xO_3$ film and a mixed valence model for $CaRu_{1-x}Mn_xO_3$ film. Ferromagnetism was also observed for layered $CaRuO_3/CaMnO_3$ film and $CaRuO_3/CaMnO_3/CaRuO_3/CaMnO_3$ multilayer film and the magnetism was explained by an interfacial exchange interaction model with magnetic Mn^{3+}, Mn^{4+}, and Ru^{5+} ions.

1. Introduction

Perovskite-type oxides have been used in a variety of electronic devices. They exhibit a variety of electric and magnetic properties, including ferroelectricity, ferromagnetism, and superconductivity. Recent developments in thin film technology opened a route to grow epitaxial multilayers comprised of oxides with different physical properties. For example, ferroelectric capacitors [1] for ferroelectric random access memory (FeRAM) and novel ferromagnet/insulator/ferromagnet structures [2,3] for a spin-polarized tunneling device have been fabricated using metallic ferromagnet $SrRuO_3$. Moreover, perovskite-type oxides have attracted renewed attention from a viewpoint of physics because various novel electric and magnetic properties due to a strong correlation between charge carrier and spin were found in perovskite-type manganites such as (Pr, Ca)MnO_3 system [4].

Among a variety of perovskite-type oxides, ferromagnetic ruthenate, $SrRuO_3$, has been practically used as a novel electrode material. However, $CaRuO_3$ has not been used practically in spite of the similarity in the crystallographic and electric properties to those of $SrRuO_3$. $CaRuO_3$ is known to be an itinerant paramagnet that is on the verge of magnetic ordering [5]. Therefore, $CaRuO_3$ readily forms magnetic order when other metal ions are doped into Ru site [6–16]. However, the mechanism of the occurrence of ferromagnetism has not been understood well. In the studies for bulk polycrystalline samples of $CaRu_{1-x}Ti_xO_3$, it was reported briefly that ferromagnetic behavior appears in the paramagnetic $CaRuO_3$ for very small Ti substitution ($x \geq 0.05$) [11,12] and, furthermore, magnetic moment is induced on Ru by Ti doping [12]. To deepen our understanding of the occurrence of ferromagnetism in $CaRu_{1-x}M_xO_3$ (M = transition metal ions) system, systematic study on samples with a variety of composition and single-crystalline samples seems necessary. In general, single crystal of $SrRuO_3$ or $CaRuO_3$ is grown by the flux method using $SrCl_2$ or $CaCl_2$ as a flux; however, it is hard task to grow a large crystal. In this case, epitaxial thin film may open a route to study intrinsic properties of ruthenates instead of using bulk single-crystalline samples. In this study, we tried epitaxial growth of $CaRu_{1-x}M_xO_3$ (M = Ti, Mn) films and multilayer films of $CaRuO_3$ and $CaMnO_3$ on $SrTiO_3$(0 0 1) substrate and investigated their crystallographic, magnetic, and electric properties.

* Corresponding author. Tel.: +81 042 759 6255; fax: +81 042 759 6523.
E-mail address: yunaga@ee.aoyama.ac.jp (Y. Nagata).

0304-8853/$ - see front matter © 2009 Elsevier B.V. All rights reserved.
doi:10.1016/j.jmmm.2009.06.031

2. Experimental details

Thin films of $CaRu_{1-x}M_xO_3$ (M = Ti, Mn) systems were prepared on a $SrTiO_3$ (0 0 1) substrate by the spin-coat method using metal alkoxides. A mixture of Ca-alkoxide (CaO concentration of ~3 wt%) and (Ru, M)-alkoxide (MO_2 concentration of ~3 wt%) was deposited on the $SrTiO_3$(0 0 1)-substrate using a spinner (5000 rpm, 10 s.) [17] and heated at 300 °C for one minute. Spin coating and heat treatment were repeated several times to attain the desired film thickness. After finishing coating, the substrate was heated at 900 °C in an ambient atmosphere for 30 min to cause the epitaxial growth of the $CaRuO_3$ film. The thickness of the film was measured by profilometry, and the morphology of the film was investigated using an optical microscope and a scanning electron microscope (SEM). The crystal structure of the film was characterized by X-ray diffraction (XRD) using CuKα radiation and the crystal structure refinement was performed by the Rietveld method. The texture of the film was characterized by XRD pole-figure, reciprocal map, and reflection high-energy electron diffraction (RHEED) measurements. Transmission electron microscopy was used to characterize a cross section of the film. Magnetic properties were characterized by a SQUID magnetometer at temperature ranging between 5 and 300 K under applied magnetic fields up to 10 kOe. The electrical resistivity was measured by a DC four-probe method. Electrical contacts were established by using gold wires (50 mm) and silver paste.

3. Results and discussion

Figs. 1(a) and 2(a) show the XRD profile for a $CaRu_{1-x}Ti_xO_3$ (hereafter referred to as CRTO) and $CaRu_{1-x}Mn_xO_3$ (hereafter referred to as CRMO) films grown on $SrTiO_3$ (0 0 1) substrate (hereafter referred to as STO(0 0 1) substrate). The insets of the figures are typical surface morphologies of $CaRu_{1-x}Ti_xO_3$ and $CaRu_{1-x}Mn_xO_3$ films. The $CaRu_{1-x}Ti_xO_3$ films have rather smooth surface; however, some roughness is observed in the surface of $CaRu_{1-x}Mn_xO_3$ films. No trace of the precipitation of the second phase was observed. The profile consists of the diffraction peaks of the (0 0 l) planes of $CaRu_{1-x}M_xO_3$ (M = Ti, Mn) films and the (0 0 l) planes of the STO substrate, indicating that the (0 0 l) planes of $CaRu_{1-x}M_xO_3$ films are parallel to the (0 0 l) planes of the STO substrate. This results indicate that the $CaRu_{1-x}M_xO_3$ films grow so as to orient the c-axis perpendicular to the (0 0 1) plane of the STO substrate. An orthorhombic (space group *Pbnm*) lattice constant c was obtained from the XRD data for the $CaRu_{1-x}M_xO_3$ films. Figs. 1(b) and 2(b) show the lattice constant c of the films and those of polycrystals as a function of the dopant content. Although the lattice constant c is slightly larger than those of the polycrystals for small M doping, the lattice constants of the film and polycrystal show almost same composition dependence. The lattice dilation observed for films with small M dopant cannot be attributed to the lattice mismatch because the tensile stress in-plane will lead to a compressive strain out-of-plane. Differential thermal expansion of the $CaRu_{1-x}M_xO_3$ films and the STO substrate may cause the lattice dilation; however, the explicit reason for the lattice dilation is presently unclear. The lattice constants of CRTO and CRMO systems decrease when Ti or Mn is substituted for Ru. The ionic radii of Ti^{4+} (0.0605 nm) and Mn^{4+} (0.053 nm) are smaller than that of Ru^{4+} (0.062 nm); this fact indicates that Ti or Mn as expected replaces the Ru site. The lattice constant of CRTO system shows almost linear decrease following Vegard's law; however, that of CRMO deviates considerably from linearity. In particular, the deviation observed for the CRMO system has been explained assuming a mixed

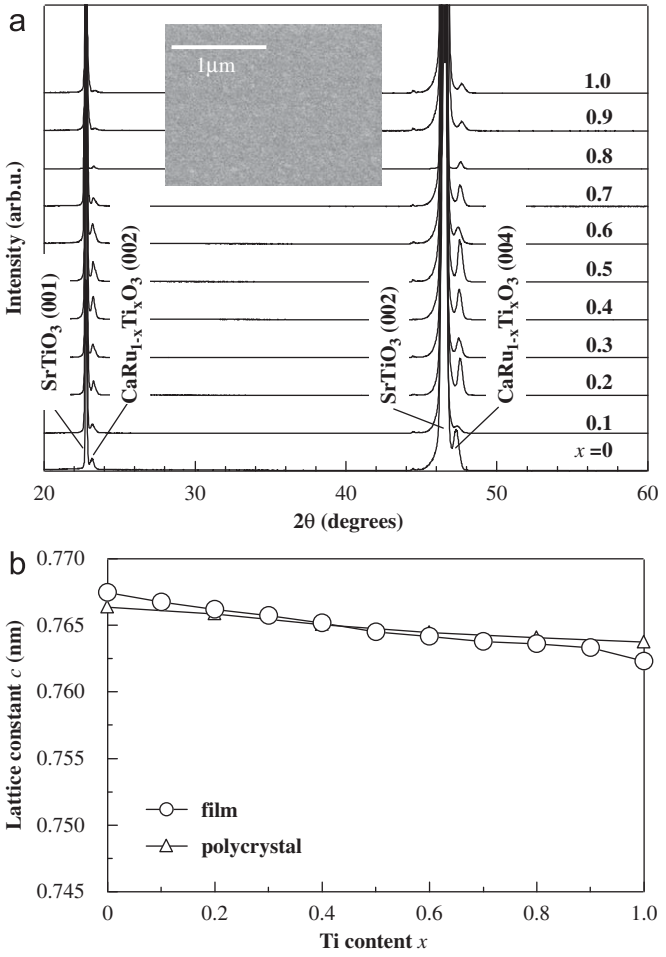

Fig. 1. (a) XRD profiles and (b) Ti-content dependence of the lattice constant c for $CaRu_{1-x}Ti_xO_3$ films grown on $SrTiO_3$(0 0 1) substrate. The inset of (a) shows the SEM image of the film surface.

valence state of Ru^{4+}, Ru^{5+}, Mn^{3+}, and Mn^{4+} ions [15]. The reason for the small linear decrease in the lattice constant of CRTO is discussed later after showing the results of the magnetic measurements.

A transmission electron microscope (TEM) image of the cross section of a $CaRu_{0.5}Ti_{0.5}O_3$ (hereafter referred to as CRTO-0.5) film on STO(0 0 1) substrate is shown in Fig. 3(a). The lattice image indicates that CRTO-0.5 layer grows epitaxially on the STO substrate. The lattice spacing of 0.38 nm was obtained for CRTO-0.5 layer. As shown in the figure, this value agrees well with the lattice constant of pseudocubic lattice (space group $Pm3\bar{m}$) of CRTO-0.5. Since the lattice spacing of the CRTO-0.5 layer is very close to the lattice constant of the cubic STO substrate (a ~0.39 nm), CRTO-0.5 layer seems to grow pseudomorphically in such a manner that its cubic axes coincide with those of the STO substrate. Possible growth model is shown in Fig. 3(b). The texture of the $CaRu_{1-x}Ti_xO_3$ films was investigated by the reciprocal lattice map and pole-figure measurements with respect to a given crystallographic orientation. Fig. 3(c) shows the reciprocal lattice map around the (0 0 2) Bragg peak of the STO substrate. The spot of the (0 0 4) plane of CRTO-0.5 film is observed. This suggests that the pseudocubic axes of the CRTO-0.5 layer are parallel to the cubic axes of the STO substrate. The pole figure was measured at a Bragg angle to record the (1 1 2) reflections. Fig. 3(d) shows the (1 1 2) pole figures of the CRTO-0.5 film grown on the STO(0 0 1) substrate. Four sharp peaks are observed, indicating that films grow while keeping the [0 0 1] direction normal to the (0 0 1)